ISSN 1063-7745, Crystallography Reports, 2011, Vol. 56, No. 6, pp. 941–946. © Pleiades Publishing, Inc., 2011.
Original Russian Text © V.G. Kohn, M.A. Orlov, 2011, published in Kristallografiya, 2011, Vol. 56, No. 6, pp. 1007–1012.

Dedicated to the memory of N.V. Belov

Theoretical Analysis of the Possibilities of Zernike Phase Contrast Method in Hard X Rays for Nondestructive Imaging of Micropipes in a Silicon Carbide Single Crystal

V. G. Kohn[a] and M. A. Orlov[b]

[a] *National Research Center Kurchatov Institute, pl. Akademika Kurchatova 1, Moscow, 123182 Russia*
e-mail: kohnvict@yandex.ru

[b] *Moscow State University, Moscow, 119991 Russia*

Received May 16, 2011

Abstract—The possibilities of using Zernike phase contrast in hard X rays for imaging micropipes in a silicon carbide single crystal are analyzed by numerical simulation. Calculations are performed for the experimental conditions characteristic of third-generation synchrotron radiation sources. A scheme is considered where the focusing element is a parabolic refracting lens and the phase-shifting element is mounted at the point of the source image. It is shown that micropipe cross sections by a beam with a longitudinal diameter reaching 10 μm are imaged by the lens without distortions. At the same time, the lens makes it possible to magnify the image several tens of times. The cross sections that are significantly elongated along the beam are imaged with artifacts; however, their structure can also be recovered. It is shown that polychromaticity of radiation does not significantly affect the object imaging.

DOI: 10.1134/S1063774511060137

INTRODUCTION

Silicon carbide (SiC) is a promising material of semiconductor electronics which is superior over silicon in many parameters (thermal conductivity, breakdown voltage, etc.). The growth of SiC crystals is accompanied by the formation of peculiar lattice defects which are called micropipes. These are strongly elongated cylindrical pores with variable cross sections with diameters ranging from a few tenths of a micrometer to several micrometers. Micropipes can be considered screw dislocations with very large values of the Burgers vector [1].

The micropipes in SiC crystals significantly deteriorate the functioning of devices based on them. To reduce the density of micropipes, nondestructive methods should be developed to study their structure and properties. Micropipes are investigated by the same methods as dislocations: the scanning electron microscopy of etch pits on the surface, X-ray topography [2] and optical microscopy. The most direct and nondestructive technique for studying the structure of micropipes directly in the sample bulk is the X-ray in-line phase contrast method [3–7]. However, this technique is not efficient for studying micropipes with a cross-sectional diameter of about 1 μm or smaller [8].

In this study we performed a computer simulation of the experiments on imaging micropipes in a SiC single crystal using the Zernike phase contrast method. A parabolic refracting lens was used as an objective, and a phase-shifting element was placed at the point of source image. Cylindrical micropipes with a constant diameter at some portion of their length were considered. In this case, the micropipe cross section by an X-ray beam propagating along the z axis has an elliptical shape, and it is sufficient to perform a calculation for only the x direction, which is perpendicular to the axis of a micropipe in its real two-dimensional image. For brevity, we will characterize the micropipe by its elliptical cross section in the (x, z) plane for which the calculation is carried out.

The specificity of the small micropipe cross section is as follows: first, the phase shift introduced by this micropipe into the incident beam becomes small and, second, the Fraunhofer diffraction conditions are satisfied when the transverse micropipe diameter is smaller than the diameter of the first Fresnel zone. Concerning the diffraction in the *in-line* scheme (standard phase contrast), the image is in the form of Fresnel zones, the sizes of which depend on the sample–detector distance, and the information about the micropipe cross-sectional sizes can be derived from only the image contrast. In this case, one can determine only the area of the cross section and not its radii along and across the beam separately.

The problem of completely determining the cross-sectional diameters can be solved by applying the well-known method of the Zernike phase contrast for visible light [9] to the X-ray range. This method was proposed in 1934; currently, it is widely used in optical studies of the structure of weakly absorbing micrometer-sized samples (biological cells, etc.). Its essence is

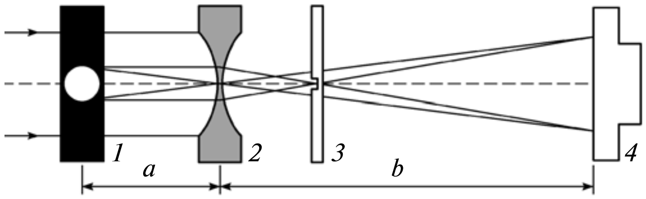

Fig. 1. Schematic of the Zernike phase contrast method for studying micropipes in silicon carbide (a synchrotron radiation beam with a very low divergence is incident from the left): (*1*) object (SiC crystal with a pore at the center), (*2*) refracting lens, (*3*) phase-shifting element (hole), and (*4*) coordinate detector. The distances a and b are related by the lens formula: $a^{-1} + b^{-1} = F^{-1}$. As a result, the image is inverted and enlarged by a factor of M, where $M = b/a$.

as follows: a transparent object, which hardly changes the intensity of radiation incident on it, is visualized by placing a quarter-wave phase-shifting plate in the objective focus. In this case, the contrast is equal to the doubled phase shift introduced by the object.

The Zernike phase contrast method is rather widely used in optical studies. However, only few experiments on its application in the X-ray range have been carried out to date [10–12]; a zone plate served as an objective in these experiments. A zone plate is known to have many focusing orders, and only a 40% incident beam intensity is used to form the first-order image. At the same time, the refracting lens completely focuses the beam and, therefore, can provide a better resolution [13]. One advantage of the Zernike method over the in-line phase contrast technique is that in the former case the detector directly yields an object image rather than a hologram (the latter must be interpreted). In addition, the refracting lens makes it possible to magnify an image by several tens of times; this is a significant advantage, because the resolution of the best coordinate detectors does not exceed several tenths of a micrometer.

SCHEMATIC OF THE NUMERICAL EXPERIMENT AND THE CALCULATION METHOD

A schematic of the experiment is shown in Fig. 1. We will denote the distances from the X-ray source to the object, focusing lens, source focus, and the coordinate detector as r_1, r_2, r_3, and r_4, respectively. Object 1 is located at the distance $r_2 - r_1 = a$ from the X-ray refracting lens (object 2). A phase-shifting element (object 3) is placed at the source image point ($r_3 = r_2 + F/(1 - F/r_2)$, which is determined from the lens formula (here, F is the lens focal distance). A detector (object 4) is located at the distance $r_4 - r_2 = b$ from the lens; the distances a and b are related by the lens formula: $a^{-1} + b^{-1} = F^{-1}$. As a result, the image is inverted and magnified by a factor of M, where $M = b/a$.

When solving the problems of hard-X-ray propagation, the paraxial approximation is satisfied with high accuracy. The X-ray propagation in air is described using the solution of the Maxwell equation in the form of Kirchhoff integral. Let the z axis of the Cartesian coordinate system coincide with the optical axis along which the X-ray beam propagates. The problem is reduced to a calculation of the dependence of the wave-field amplitude on the transverse coordinates x and y at each point on the z axis. Note that in the transverse directions the wave field changes significantly at distances of several micrometers or smaller, whereas the characteristic range of variation in the wave field along the z axis is much larger. The polarization remains not changed in the processes under consideration; therefore, we will restrict ourselves to the scalar wave function of the field. Moreover, we will consider only one-dimensional objects homogeneous along the y axis.

Let $E_1(x)$ be the wave function at the point z_1. Then the wave function $E(x)$ at the point z is determined (provided that there are no objects between z_1 and z) as

$$E(x) = \int dx_1 P(x - x_1, z - z_1) E_1(x_1), \qquad P(x, z) = \frac{1}{(i\lambda z)^{1/2}} \exp\left(i\pi \frac{x^2}{\lambda z}\right). \tag{1}$$

Here, $P(x, z)$ is the Kirchhoff propagator in the paraxial approximation and λ is the X-ray wavelength. Concerning the objects, if their longitudinal sizes do not differ much from transverse, the change in the beam trajectory during transmission through the object can be neglected, because the scattering angles are fairly small (generally several tens of microradians). When describing the interaction of radiation with an object, one can neglect the longitudinal object length and consider it to be planar and located in the plane passing through the midpoint of its length. However, when describing the radiation transport, the volume covered by the object length is taken into account as an empty space. Sometimes this is an important factor, for example, for a compound refracting lens, the length of which is comparable with its focal distance. Thus, to describe the interaction of radiation with an object, the wave function of the radiation field is multiplied by the so-called transmission function

$$T(x) = \exp\left(-i[\delta - i\beta]\frac{2\pi}{\lambda} t(x)\right), \tag{2}$$

where $t(x)$ is a local change in the object thickness along the z axis, provided that the object consists of one material, and δ and β are the real and imaginary parts of the complex refractive index $n = 1 - \delta + i\beta$ of this material.

The calculation starts from the point source. The wave function in the source plane can formally be taken in the form of the δ function: $E_0(x) = \delta(x)$. Substituting it into (1), we directly obtain the wave function before the object under study in the form of a Kirchhoff propagator: $E_1(x) = P(x, r_1)$. Furthermore it is necessary to multiply the wave function by the transmission function of the object with the specific form of the dependence $t(x)$ taken into account and then apply (1) again:

$$E_2(x) = \int dx_1 P(x - x_1, r_2 - r_1) T(x_1) E_1(x_1). \quad (3)$$

In the first calculation, r_2 is equal to the distance from the source to the focusing lens (Fig. 1). In this study we considered only elliptical cross sections of micropipe; their transmission function has the form

$$t(x) = 2R_1\left(1 - \frac{x^2}{R_2^2}\right)^{1/2}, \quad (4)$$

where R_1 and R_2 are the cross-sectional radii along and across the beam, respectively. Then the calculation must be repeated with a new object in the form of a focusing lens; to this end, the replacements $r_2 \to r_3$ and $r_1 \to r_2$ must be made in (3). For a biconcave refracting parabolic lens, we have

$$t(x) = \frac{x^2}{R}, \quad (5)$$

where R is the radius of curvature at the parabola vertex. Note that the infinite integration limits are effectively cut off due to the absorption in the lens, because the lens is fairly thick at the aperture edges. In the third calculation, the object is the phase-shifting element with a diameter of the same order of magnitude as the beam diameter in the lens focus. In this case, the replacements $r_2 \to r_4$ and $r_1 \to r_3$ must be made in (3). In optical studies a cylindrical plate is used as a phase-shifting element; however (see below), to study pores in a material in the X-ray range, it is more convenient to use a cylindrical hole. We consider an ideal phase-shifting element: a hole in a nonabsorbing material, because a consideration of absorption does not significantly change the results. Thus, in our case, $T(x) = 1$ at $|x| > D/2$ and

$$T(x) = \exp\left(i\frac{\pi}{2}\right) \quad (6)$$

at $|x| \le D/2$, where D is the hole diameter.

Integral (3) is a convolution of two complex functions, and it is convenient to calculate it using a Fourier transform. First we calculated the Fourier transform of the product of functions of the argument x_1; then it was multiplied by the Fourier transform of the Kirchhoff propagator, which has the analytical form $P(q, r) = \exp(-i\lambda rq^2/4\pi)$; and, finally, the inverse Fourier transform was calculated. The latter was performed using fast Fourier transform procedure [14].

The calculations were performed for the standard parameters of third-generation synchrotron sources, specifically the source–object distance $r_1 = 50$ m and the source size $S_0 = 50$ μm. The objective was a compound parabolic beryllium lens composed of $N = 60$ elements with radii of curvature $R = 50$ μm; the lens focal distance was 31.4 cm. The incident radiation energy was assumed to be $E = 16$ keV. The source is phase-incoherent; i.e., the radiation from each of its points has an independent phase. Since the source transverse size is S_0, its image in the focus is $S = S_0(r_3 - r_2)/(r_1 + r_2)$. The source sizes were taken into account by calculating the convolution of the intensity distribution for a point source with a Gaussian curve, the half-width of which is $S_d = S_0(r_4 - r_2)/(r_1 + r_2)$.

To select an object image in a pure form in experiments, a special procedure is often used: the image is recorded in the absence of the object and then with the object, after which the first image is subtracted from the second one. In [13], where the phase-shifting element was a cylindrical plate, the image of convex silicon objects was above the background level (it had a positive contrast) after this procedure. Since we use a hole instead of a plate, it is pores in the material rather than convex objects that must be imaged with a positive contrast.

It was noted in [13] that the quality of image objects is significantly deteriorated in the case of transverse shift of objects from the aperture center if a refracting lens is used as an objective. It was found that the image can easily be recovered by dividing the intensity profile formed by the lens by the absorption function of the lens: $\exp(-A[4\pi x^2/\lambda R_0]\beta)$, where $\beta = 5.19 \times 10^{-10}$ is the absorption index of beryllium; $R_0 = R/N$ is the effective radius of curvature of the lens; and A is the correction coefficient, which only slightly differs from unity. The use of this procedure makes it possible to equalize not only the background, but also the contrast. Note that this procedure is not necessary if the object under study is small and located at the center of the aperture, because the central region is imaged by the lens fairly well. However, this procedure must be applied to the images of objects located at a rather large distance from the optical axis.

CALCULATION RESULTS

Imaging of Objects with a Small Longitudinal Cross Section

Let the object under study be a micropipe located at the center of the lens aperture with longitudinal and transverse cross-sectional radii $R_1 = R_2 = 0.3$ μm. Figure 2 shows how the cross section of this micropipe is imaged at different magnifications. The doubled phase shift introduced by the micropipe center into the incident wave is about 0.25; specifically this value is observed on the detector at $M = 1$. With an increase in magnification, the peak width increases by a factor of M and the peak height decreases by a factor of M. This

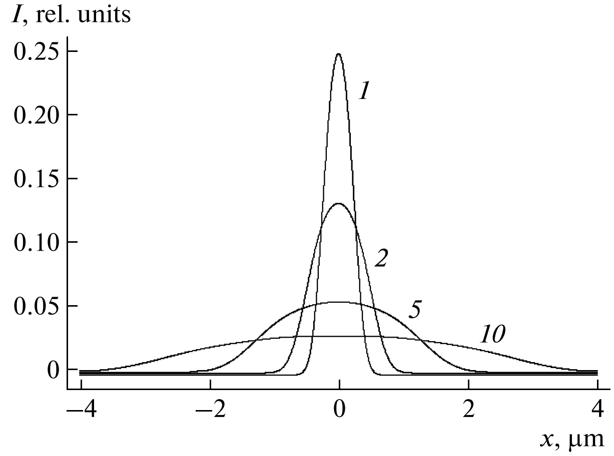

Fig. 2. Image of a micropipe with the radii $R_1 = R_2 =$ 0.3 μm at different magnifications M (indicated near the curves).

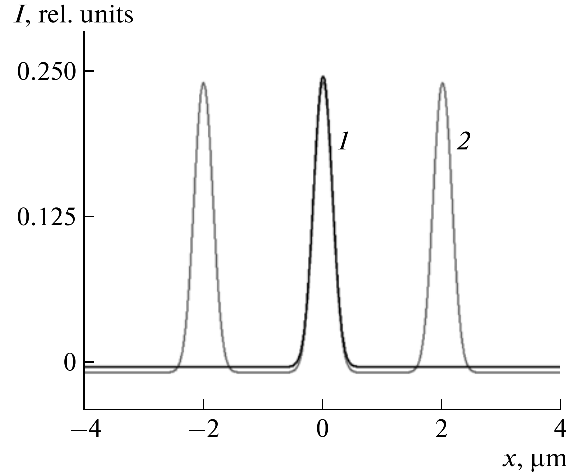

Fig. 3. Images of (*1*) a micropipe with the sizes $R_1 = R_2 =$ 0.3 μm located at the center of the aperture and (*2*) three identical micropipes; magnification $M = 1$.

property is a consequence of the energy conservation law, which is why the intensity integrated over the beam cross section should be retained. Taking into account these two circumstances, one can easily calculate the true sizes of the micropipe cross section. The small spread of the image at the edges is caused by the averaging over the source projection, the size of which linearly increases with an increase in M. An increase in the transverse cross-sectional diameter does not change the character of the above-described regularities. An increase in the longitudinal diameter up to $t \approx 10$ μm also causes no significant changes.

Note that adding new objects to existing ones affects to a certain extent the image of the latter, which manifests itself in the change in the background level. For example, Fig. 3 shows how the image changes when a micropipe with cross-sectional radii $R_1 = R_2 =$ 0.3 μm is supplemented with two similar micropipes. It can be seen that in this case the background is lowered to conserve the integral intensity. However, for micropipes with a small cross section, this does not lead to image distortions; artifacts arise only when studying objects with a large longitudinal cross section.

Thus, magnification makes it possible to observe small details in the structure of micropipe cross section, and the Zernike phase contrast method is more favorable in this context than the lensless (*in-line*) phase contrast method.

Imaging of Objects with a Large Longitudinal Cross Section

It is known that the Zernike phase contrast method in optics allows one to observe only transparent objects which introduce a small phase shift into the incident wave $\varphi \ll 1$. In this case, the transmission function of the sample $\exp(i\varphi)$, can be expanded in a Taylor series. A numerical calculation showed that, in the X-ray range, the limitation on the phase value can be got around. Let us consider the images of a series of elliptical cross sections of large pores in silicon carbide and ellipses (the cross sections of convex objects) with the same sizes (Fig. 4) in the ascending order with respect to the phase introduced by them (from right to left in Fig. 4). The last objects on the right have longitudinal diameters of 3 and 5 μm, respectively, and each subsequent object has a longitudinal diameter 5 μm larger than the previous one. The transverse diameters of all objects are in the range from 10 to 20 μm.

The calculation results show that the method proposed yields a conventional result not only for small pores (with a longitudinal cross-sectional diameter $t \approx$ 1 μm and shift phase $\varphi \approx 0.21$) but also pores with much larger longitudinal sizes (to $t \approx 10$ μm). With a subsequent increase in the longitudinal cross section, the image starts inverting and a dip (increasing in depth) arises instead of a peak. The mechanism of this (at first glance incomprehensible) phenomenon becomes clear when considering the further increase in the longitudinal size of pores: the central peak returns to the same position each time when a phase shift of 2π is accumulated in the pore, because at these values the pore transmission function takes the same values ($\exp(2\pi i) = 1$). Thus, proceeding from the total number of oscillations and the central peak height, one can determine the longitudinal size of highly elongated elliptical cross section of pores. The images of convex objects with an elliptical cross section exhibit a similar regularity; however, the corresponding oscillations show a phase delay with respect to the oscillation characteristic of pores; the first invertion in the case of objects arises at $\varphi \approx 1$. Note that, for the objects that introduce small variations in the phase φ, the dip depth is not 2φ but $2\varphi - \varphi^2$, which follows from the

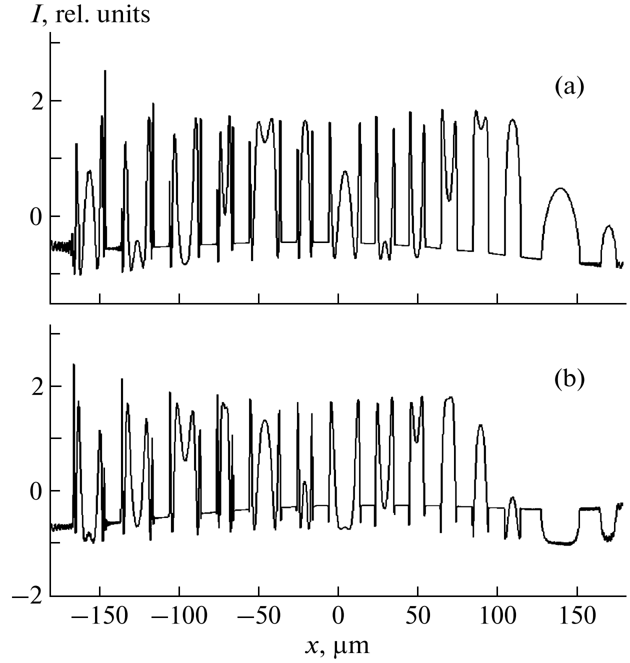

Fig. 4. Images of (a) a series of large pores and (b) a series of large objects of the same sizes.

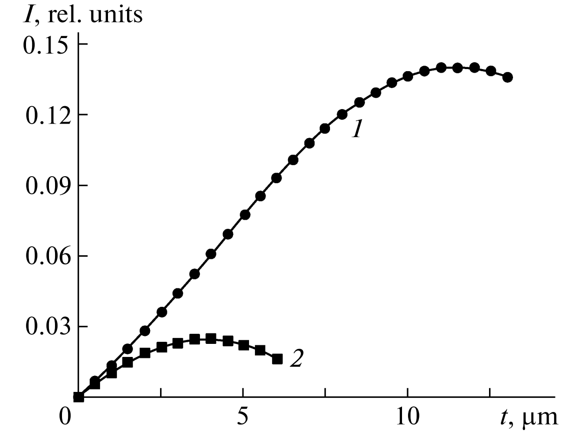

Fig. 5. Dependences of the peak height on the longitudinal diameter t of the cross section of (*1*) a pore in silicon carbide with $R_2 = 0.5$ μm and (*2*) a SiC object of the same size; magnification $M = 40$. Curve *2* is inverted.

approximate theory of the Zernike method. This is shown more clearly in Fig. 5, which demonstrates the dependence of the peak height on the longitudinal diameter of the cross sections of pore and object with $R_1 = R_2 = 0.5$ μm (for magnification, $M = 40$). It follows from Fig. 5 that, when imaging pores, the proportionality of the peak height to the phase shift introduced by the pore is retained in a much wider range of thicknesses t than in the case of objects. Specifically this is the reason why we used a hole as a phase-shifting element instead of plate; the application of the latter from the point of view of the Zernike method would be equivalent to the transformation of pores into objects. In addition, the hole technology is simpler. Although ideally it should have a high aspect ratio, numerical calculations show that an increase in the radius of the phase-shifting element by even several times does not lead to significant image distortions.

Influence of Spectrum on Imaging

In [5–8], micropipes in silicon carbide were investigated in a white beam without a monochromator. This measurement scheme leads to a partial loss of time coherence, but it makes it possible to record more photons and, therefore, increases the signal-to-noise ratio. In this study we considered a Gaussian spectrum with a maximum at an energy of 16 keV. The intensity profiles were calculated for 21 harmonics in the range from 6 to 26 keV with a constant step of 1 keV, after which these profiles were summed with weighting factors corresponding to the Gaussian distribution. Figure 6 shows how the image of a micropipe cross section with the transverse and longitudinal radii R_1 = 1.5 μm and R_2 = 0.5 μm, respectively, changes when polychromatic radiation with Gaussian spectrum is used. It can be seen that the transverse size of the cross section is viewed without distortions on the detector and the peak height, which characterizes the longitudinal size, changes only slightly. For objects with smaller longitudinal sizes, the deviations are even smaller; more significant discrepancies arise only for samples with highly elongated elliptical cross sections. The weak influence of the spectrum on imaging objects with a small cross section is explained by the fact that the modulus of the phase shift $|P| = (2\pi/\lambda)\delta t$, which is introduced by the sample into the incident wave, increases linearly with an increase in the radiation wavelength, because δ is proportional to λ^2 with high accuracy. As a result, the increase in the contrast at lower energies compensates for its decrease at higher energies. In addition, averaging over spectrum eliminates spurious oscillations, which arise when objects displaced from the center of the aperture are imaged. In this case, the presence of a spectrum leads to small distortions in imaging peripheral samples; however, these distortions are insignificant.

CONCLUSIONS

A numerical simulation showed that the Zernike method can be successfully used to study micropipes with submicron sizes. Micropipes must be oriented perpendicularly to the beam, because in this case they introduce the smallest phase shifts, and the image has a descriptive elliptical form. The refracting lens that is used in the Zernike method makes it possible to magnify the image several tens of times. With the magnification coefficient, the height of the peak on the detector, and its transverse size known, one can easily

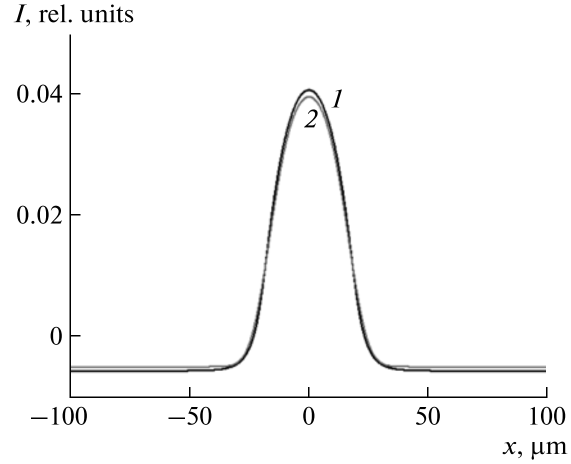

Fig. 6. Images of a micropipe with the transverse diameter $R_1 = 1.5$ μm and $R_2 = 0.5$ μm obtained in (*1*) a monochromatic beam and (*2*) a polychromatic beam with a specified spectrum; magnification $M = 40$.

reconstruct the true sizes of the micropipe cross section. When imaging micropipes with a small cross section, it is more expedient to use a hole in a material instead of a plate as a phase-shifting element, because in this case pores with a longitudinal diameter up to $t \approx 10$ μm are imaged without distortions. Images of objects with highly elongated elliptical cross sections contain oscillations, and the object structure can be reconstructed if the total number of oscillations and the height of the central peak are known. The beam polychromaticity does not significantly affect the imaging of micropores and can be used to amplify the desired signal and reduce the background noise.

ACKNOWLEDGMENTS

This study was supported by the Russian Foundation for Basic Research, project nos. 10-02-00047-a and 09-02-12239-ofi_m.

REFERENCES

1. P. Krishna, S.-S. Jiang, and A. R. Lang, J. Cryst. Growth **71**, 41 (1985).
2. X. R. Huang, M. Dudley, W. M. Vetter, et al., J. Appl. Crystallogr. **32**, 516 (1999).
3. M. Yu. Gutkin, A. G. Sheinerman, T. S. Argunova, et al., Phys. Rev. B **76**, 064117 (2007).
4. M. Yu. Gutkin, A. G. Sheinerman, M. A. Smirnov, et al., Appl. Phys. Lett. **93**, 151905 (2008).
5. V. G. Kohn, T. S. Argunova, and H. J. Jung, Appl. Phys. Lett. **91**, 171901 (2007).
6. T. S. Argunova, V. G. Kohn, J. W. Jung, and H. J. Jung, Phys. Status Solidi A **206** (8), 1833 (2009).
7. T. S. Argunova, V. G. Kon, and Ho. Je. Jung, Poverkhnost **12**, 1 (2008).
8. V. G. Kon, T. S. Argunova, and Ho. Je. Jung, Poverkhnost **1**, 3 (2011).
9. F. Zernike, Z. Tech. Phys. **16**, 454 (1935).
10. G. Schmahl, D. Rudolph, P. Guttmann, et al., Rev. Sci. Instrum. **88** (2), 1282 (1995).
11. H. Yokosuka, N. Watanabe, T. Ohigashi, et al., J. Synchrotron Radiat. **9**, 179 (2002).
12. Y. S. Chu, J. M. Yi, F. De Carlo, et al., Appl. Phys. Lett. **92**, 103119 (2008).
13. V. G. Kon and M. A. Orlov, Poverkhnost **11**, 76 (2010).
14. http://alglib.sources.ru/fft.

Translated by Yu. Sin'kov